

# Spin-Fluctuation-Driven Orbital Nematic Order in Ru-Oxides: Self-Consistent Vertex Correction Analysis for Two-Orbital Model

Yusuke OHNO<sup>1</sup>, Masahisa TSUCHIIZU<sup>1</sup>, Seiichiro ONARI<sup>2</sup>, and Hiroshi KONTANI<sup>1</sup>

<sup>1</sup> *Department of Physics, Nagoya University, Furo-cho, Nagoya 464-8602, Japan.*

<sup>2</sup> *Department of Applied Physics, Nagoya University, Furo-cho, Nagoya 464-8603, Japan.*

(Dated: March 15, 2021)

To reveal the origin of the “nematic electronic fluid phase” in  $\text{Sr}_3\text{Ru}_2\text{O}_7$ , we apply the self-consistent vertex correction analysis to the  $(d_{xz}, d_{yz})$ -orbital Hubbard model. It is found that the Aslamazov-Larkin type vertex correction causes the strong coupling between spin and orbital fluctuations, which corresponds to the Kugel-Khomskii spin-orbital coupling in the local picture. Due to this mechanism, orbital nematic order with  $C_2$  symmetry is induced by the magnetic quantum criticality in multiorbital systems, whereas this mechanism is ignored in the random-phase approximation. The present study naturally explains the intimate relation between the magnetic quantum criticality and the nematic state in  $\text{Sr}_3\text{Ru}_2\text{O}_7$  and Fe-based superconductors.

Keywords:  $\text{Sr}_3\text{Ru}_2\text{O}_7$ , orbital nematic order, vertex correction, quantum criticality

Recently, emergence of orbital (or quadrupole) order or orbital fluctuations in multiorbital systems has been attracting great attention. In heavy-fermion systems,  $\text{CeB}_6$  exhibits non-magnetic quadrupole order [1], and the hidden-order phase in  $\text{URu}_2\text{Si}_2$  [2, 3] is expected as quadrupole or higher-rank multipole order. As for  $d$ -electron systems, Fe-based superconductors exhibit “non-magnetic” orthorhombic structure transition at  $T = T_S$  as well as the nematic order, which indicates the occurrence of the ferro-orbital polarization  $n_{xz} \neq n_{yz}$  [4, 5]. Large softening of shear modulus  $C_{66}$  above  $T_S$  indicates the existence of strong orbital fluctuations [6–8].

The quantum critical phenomenon in bilayer perovskite  $\text{Sr}_3\text{Ru}_2\text{O}_7$  is very unique in that both spin and charge degrees of freedom are intimately related [9–12]. The band structure of  $\text{Sr}_3\text{Ru}_2\text{O}_7$  is composed of the  $t_{2g}$ -orbital ( $d_{xz}$ ,  $d_{yz}$ ,  $d_{xy}$  orbitals) of Ru ions. Both the  $T$ -linear resistivity [9] and the NMR result  $1/T_1T \propto T^{-1}$  [11] are observed below 20 K under the magnetic field  $H_c \approx 7.8$  Tesla. These non-Fermi liquid behaviors indicate the emergence of “antiferromagnetic quantum criticality (AFM-QC)” at  $H \approx H_c$ , although no long-range magnetic order is observed till 0.1 K [10, 11].

Under the critical field  $H \approx H_c$ , moreover,  $\text{Sr}_3\text{Ru}_2\text{O}_7$  exhibits a novel “non-magnetic nematic electronic fluid phase” below 1 K, which is confirmed by the large anisotropy of in-plane resistivity [10]. As a possible origin, the Pomeranchuk instability of the Fermi surfaces (FSs) in the single-band Hubbard model had been studied using the renormalization group method [13, 14] and the perturbation theory [15]. Also, the orbital polarized state has been studied based on multiorbital Hubbard models, using the mean-field-level approximation (MFA) [16–18]. However, many of these studies do not prove the stability of the nematic order against antiferro-spin/orbital order driven by the nesting of the FS. Especially, the key question — why the non-magnetic nematic order occurs only near the AFM-QC in  $\text{Sr}_3\text{Ru}_2\text{O}_7$  — has

been still unclear.

The nematic order in Fe-based superconductors also attracts increasing attention, and it would offer us useful hints in the study of  $\text{Sr}_3\text{Ru}_2\text{O}_7$ . Since it cannot be explained in the MFA analysis, the spin nematic order due to the order-by-disorder mechanism had been proposed [6, 19]. However, it could not be applied to  $\text{Sr}_3\text{Ru}_2\text{O}_7$  since the incommensurate spin fluctuations are realized. On the other hand, we have recently revealed that the vertex correction (VC), which describes the many-body effect beyond the MFA, induces strong ferro-orbital fluctuations [20, 21]. Then, it is highly required to analyze the significance of the VC in Ru-oxides.

In this paper, we study the origin of nematic phase in  $\text{Sr}_3\text{Ru}_2\text{O}_7$  based on the two-orbital Hubbard Hamiltonian. We utilize the self-consistent VC (SC-VC) method, which was recently applied to Fe-based superconductors successfully, and reveal that the “orbital Pomeranchuk instability” is generally induced near AFM-QC, owing to the spin-orbital coupling given by the VC. The present study predicts the realization of orbital nematic order near the field-induced AFM-QC in  $\text{Sr}_3\text{Ru}_2\text{O}_7$ .

The bandstructure of  $\text{Sr}_3\text{Ru}_2\text{O}_7$  is rather complex because of the tilting of  $\text{RuO}_6$  octahedra. Therefore, we study the simplified  $(d_{xz}, d_{yz})$ -orbital model to grasp the essential mechanism of the orbital nematicity:

$$H = \sum_{\mathbf{k}; \sigma=\uparrow, \downarrow; \mu, \nu=1, 2} \xi_{\mathbf{k}}^{\mu\nu} c_{\mathbf{k}, \mu, \sigma}^\dagger c_{\mathbf{k}, \nu, \sigma} + H_C, \quad (1)$$

where  $\mu, \nu = 1, 2$  represents the  $d$ -orbital;  $1 = xz$  and  $2 = yz$ . This model describes the  $\alpha$  FS and  $\beta$  FS of Ru-oxides, and it was analyzed in the study of anomalous/spin Hall effect [22]. Hereafter, we promise that  $x, y$ -axes are along the nearest Ru-Ru bond directions. Then, the intra- and inter-orbital hoppings are given as  $\xi_{\mathbf{k}}^{11} = -2t \cos k_x$ ,  $\xi_{\mathbf{k}}^{22} = -2t \cos k_y$ , and  $\xi_{\mathbf{k}}^{12} = 4t' \sin k_x \sin k_y$ . In this paper, we put  $(t, t') = (1, 0.1)$ . The FSs for the electron filling  $n = 2$  are shown in Fig. 1 (a). In  $\text{Sr}_3\text{Ru}_2\text{O}_7$ ,

$(\alpha, \beta)$  FSs split into the bonding  $(\alpha_1, \beta_1)$  FSs and the antibonding  $(\alpha_2, \beta_2)$  FSs by large interlayer hoppings. The electron filling of  $(\alpha_1, \beta_1)$  FSs is about 3.2 – 3.5 [16, 17], and we set  $n = 3.3$  in this study.  $H_C$  represents the multi-orbital Coulomb interaction composed of intra (inter) orbital interaction  $U$  ( $U'$ ) and the exchange interaction  $J$ . [21]. Hereafter, we put  $U = U' + 2J$ .

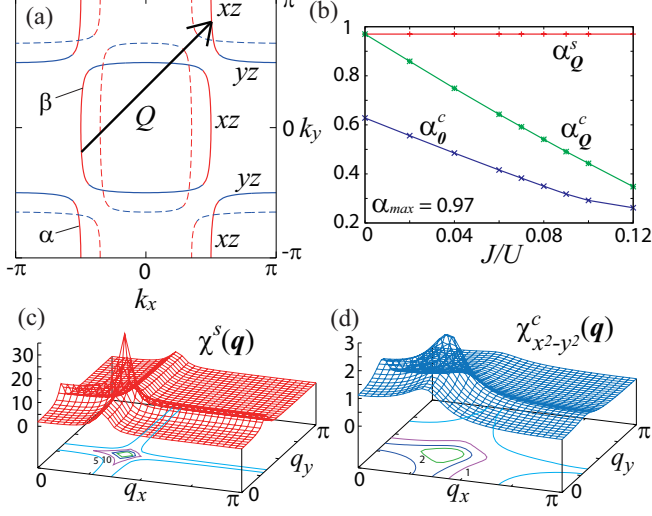


FIG. 1: (color online) (a) FSs of the two-orbital model for  $n = 2$ . The colors correspond to 1 =  $xz$  (red) and 2 =  $yz$  (blue). The arrow represents the  $xz$  intra-orbital nesting vector. The dashed lines represent the deformed FSs for  $\langle \hat{O}_{x^2-y^2} \rangle < 0$ . (b)  $\alpha_Q^s$ ,  $\alpha_Q^c$  and  $\alpha_0^c$  for  $n = 3.3$  in the RPA. (c)  $\chi^s(\mathbf{q})$  and (d)  $\chi^q(\mathbf{q})$  obtained by the RPA.

In the present model, the susceptibility for the charge (spin) channel is given by the following  $4 \times 4$  matrix form in the orbital basis:

$$\hat{\chi}^{c(s)}(\mathbf{q}) = \hat{\chi}^{\text{irr},c(s)}(\mathbf{q})(1 - \hat{\Gamma}^{c(s)}\hat{\chi}^{\text{irr},c(s)}(\mathbf{q}))^{-1}, \quad (2)$$

where  $\mathbf{q} = (\mathbf{q}, \omega_l = 2\pi l/T)$ , and  $\hat{\Gamma}^{c(s)}$  represents the Coulomb interaction for the charge (spin) channel composed of  $U$ ,  $U'$  and  $J$  given in Refs. [21]. The irreducible susceptibility is

$$\hat{\chi}^{\text{irr},c(s)}(\mathbf{q}) = \hat{\chi}^0(\mathbf{q}) + \hat{X}^{c(s)}(\mathbf{q}), \quad (3)$$

where  $\chi_{ll',mm'}^0(\mathbf{q}) = -T \sum_p G_{lm}(\mathbf{p} + \mathbf{q})G_{m'l'}(\mathbf{p})$  is the bare bubble,  $\mathbf{p} = (\mathbf{p}, \epsilon_n = (2n+1)\pi T)$ , and the second term is the VC that is neglected in the RPA.

In the present discussion, it is convenient to consider the quadrupole susceptibilities:  $\chi_\gamma^c(\mathbf{q}) \equiv \sum_{ll',mm'} O_\gamma^{l,l'} \chi_{ll',mm'}^c(\mathbf{q}) O_\gamma^{m',m}$ , where  $O_\gamma^{l,m} = \langle l | \hat{O}_\gamma | m \rangle$  is the matrix element of the  $\gamma$ -quadrupole operator. Non-zero matrix elements of the quadrupole operators are  $O_{x^2-y^2}^{1,1} = -O_{x^2-y^2}^{2,2} = 1$  and  $O_{xy}^{1,2} = O_{xy}^{2,1} = 1$  [21], while  $\hat{O}_{xz,yz} = \hat{0}$  in the present Hilbert space.

The divergence of  $\chi_{x^2-y^2}^c(\mathbf{0})$  immediately leads to the ferro-quadrupole order  $\langle \hat{O}_{x^2-y^2} \rangle = n_{xz} - n_{yz} \neq 0$ , resulting in the “nematic” deformation of the FSs shown in the

dashed lines in Fig. 1 (a). The director of the nematicity is along the Ru-Ru bond direction, which is consistent with experiments. In case of  $\langle \hat{O}_{xy} \rangle \neq 0$ , the director is rotated by  $45^\circ$ .

Here, we introduce the charge (spin) Stoner factor  $\alpha_{\mathbf{q}}^{c(s)}$ , which is the largest eigenvalue of  $\hat{\Gamma}^{c(s)}\hat{\chi}^{\text{irr},c(s)}(\mathbf{q})$  at  $\omega_l = 0$ : Then, the quadrupole (spin) susceptibility is enhanced in proportion to  $(1 - \alpha_{\max}^{c(s)})^{-1}$ , where  $\alpha_{\max}^{c(s)} \equiv \max_{\mathbf{q}} \{\alpha_{\mathbf{q}}^{c(s)}\}$ . Since  $J > 0$  in real systems, spin fluctuations are always dominant ( $\alpha_{\max}^s > \alpha_{\max}^c$ ) in the RPA as shown in Fig. 1 (b): This figure shows the  $J/U$ -dependences of  $\alpha_Q^s$ ,  $\alpha_Q^c$  and  $\alpha_0^c$  in the RPA, where  $U$  is determined by the condition  $\alpha_Q^s(U) = 0.97$ . In the SC-VC method, however, the opposite relation  $\alpha_{\max}^s \lesssim \alpha_{\max}^c$  can be realized even for  $J/U \lesssim 0.1$  because of large  $\hat{X}^c(\mathbf{q})$ .

First, we perform the RPA calculation for  $n = 3.3$  and  $T = 0.05$ , using  $64 \times 64$   $\mathbf{k}$ -meshes. The unit of energy is  $t = 1$ . Figure 1 (c) shows the spin susceptibility  $\chi^s(\mathbf{q}) = \sum_{l,m} \chi_{ll,mm}^s(\mathbf{q})$  and the (d) quadrupole susceptibility  $\chi_{x^2-y^2}^c(\mathbf{q})$  for  $J/U = 0.06$ . The Stoner factors are  $\alpha_{\max}^s = 0.97$ ,  $\alpha_Q^c = 0.64$ , and  $\alpha_0^c = 0.42$ ; see Fig. 1 (b). Both  $\chi^s(\mathbf{q})$  and  $\chi_{x^2-y^2}^c(\mathbf{q})$  have peaks at  $(q^*, q^*)$ , where  $q^* = 0.31\pi$ . Thus, the RPA cannot explain the nematic transition that requires the divergence of  $\chi_{x^2-y^2}^c(\mathbf{0})$ .

In the next stage, we study the role of VC due to the Maki-Thompson (MT) and Aslamazov-Larkin (AL) terms shown in Fig. 2 (a) of Ref. [20]. They are given by the Ward identity  $\Gamma^I = \delta \Sigma_{\text{FLEX}} / \delta G$  using the FLEX self-energy. Moreover, they correspond to the first-order mode-coupling corrections to the RPA susceptibility: The intra- (inter-) bubble correction gives the MT (AL) term [23]. In single-orbital models, these VCs had been studied by the self-consistent-renormalization (SCR) theory [23]. However, significant role of the AL-type VC in multi-orbital systems had been overlooked until recently [20].

The charge AL term  $\hat{X}^{\text{AL},c}(\mathbf{q}) \equiv \hat{X}^{\text{AL},\uparrow,\uparrow}(\mathbf{q}) + \hat{X}^{\text{AL},\uparrow,\downarrow}(\mathbf{q})$  is given in eq. (5) of Ref. [20]. Also, the  $ll',mm'$  component of the spin AL term  $\hat{X}^{\text{AL},s}(\mathbf{q}) \equiv \hat{X}^{\text{AL},\uparrow,\uparrow}(\mathbf{q}) - \hat{X}^{\text{AL},\uparrow,\downarrow}(\mathbf{q})$  is given as

$$\begin{aligned} \frac{T}{2} \sum_k \sum_{a \sim h} \Lambda_{ll',ab,ef}(q;k) \{ & V_{ab,cd}^s(k+q) V_{ef,gh}^c(-k) \\ & + V_{ab,cd}^c(k+q) V_{ef,gh}^s(-k) \} \Lambda'_{mm',cd,gh}(q;k) \\ & + 2V_{ab,cd}^s(k+q) V_{ef,gh}^s(-k) \Lambda''_{mm',cd,gh}(q;k), \end{aligned} \quad (4)$$

where  $\hat{V}^{s,c}(\mathbf{q}) \equiv \hat{\Gamma}^{s,c} + \hat{\Gamma}^{s,c} \hat{\chi}^{s,c}(\mathbf{q}) \hat{\Gamma}^{s,c}$ .  $\hat{\Lambda}(q;k)$  is the three-point vertex [20], and  $\Lambda'_{mm',cd,gh}(q;k) \equiv \Lambda_{ch,mg,dm'}(q;k) + \Lambda_{gd,mc,hm'}(q;-k-q)$  and  $\Lambda''_{mm',cd,gh}(q;k) \equiv \Lambda_{ch,mg,dm'}(q;k) - \Lambda_{gd,mc,hm'}(q;-k-q)$ . Since  $\hat{X}^{\text{AL},c}(\mathbf{0}) \sim \sum_k \hat{\Lambda}(3\hat{V}^s(k)^2 + \hat{V}^c(k)^2) \hat{\Lambda}'$ , it becomes significant when either  $\hat{\chi}^c$  or  $\hat{\chi}^s$  is large, while  $\hat{X}^{\text{AL},s}$  is less important unless both  $\hat{\chi}^c$  and  $\hat{\chi}^s$  are large since  $\hat{\Lambda}'' \ll \hat{\Lambda}'$ . For this reason, in Ref. [20], we

have calculated only  $\hat{X}^c(\mathbf{q})$  by putting  $\hat{X}^s(\mathbf{q}) = 0$  for simplicity. In the present study, we also calculate both  $\hat{X}^c(\mathbf{q})$  and  $\hat{X}^s(\mathbf{q})$  self-consistently. Hereafter, we call the former (latter) the SC-VC[c] (SC-VC[all]) method. We will show that both methods give similar results.

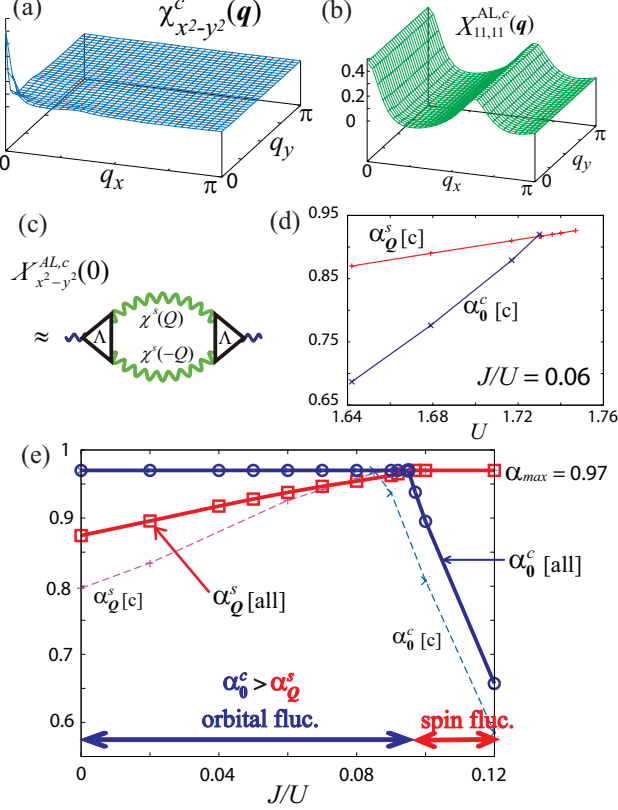


FIG. 2: (color online) (a)  $\chi_{x^2-y^2}^c(\mathbf{q})$  and (b)  $X_{11,11}^{AL,c}(\mathbf{q})$  given by the SC-VC[c] method for  $U = 1.75$  and  $J/U = 0.06$ . (c) the charge AL term. (d)  $\alpha_Q^c$  and  $\alpha_0^c$  in the SC-VC[c] method as function of  $U$  under the condition  $J/U = 0.06$ . (e)  $\alpha_Q^c$  and  $\alpha_0^c$  as function of  $J/U$  in the SC-VC[all] and SC-VC[c] methods, under the condition  $\alpha_{\max} \equiv \max\{\alpha_{\max}^s, \alpha_{\max}^c\} = 0.97$ .

First, we present the numerical results given by the SC-VC[c] method: Figure 2 (a) shows  $\chi_{x^2-y^2}^c(\mathbf{q})$  obtained for  $n = 3.3$ ,  $J/U = 0.06$  and  $U = 1.75$ , in which the Stoner factors are  $\alpha_{\max}^s = 0.93$  and  $\alpha_0^c = 0.97$ . In comparison with the RPA,  $\chi_{x^2-y^2}^c(\mathbf{q})$  is strongly enhanced by the charge AL term, while the results are almost unchanged even if MT term is dropped. Figure 2 (b) presents the momentum dependence of the charge VC,  $X_{11,11}^{AL,c}(\mathbf{q})$ , which is enhanced on lines  $q_x = 0, 2q^*$  because of the two-magnon process in Fig. 2 (c), reflecting the good nesting of the quasi one-dimensional  $xz$ -orbital bands. (Fig. 2 (c) shows a virtual decay process of an orbital into two magnons with opposite momenta  $\pm\mathbf{Q}$ .) In the same way,  $X_{22,22}^c(\mathbf{q})$  is enhanced on lines  $q_y = 0, 2q^*$ . Thus, both  $X_{11,11}^c(\mathbf{q})$  and  $X_{22,22}^c(\mathbf{q})$  give the enhancement of  $\chi_{x^2-y^2}^c(\mathbf{q})$  at  $\mathbf{q} = \mathbf{0}$ . In contrast,  $\chi_{xy}^c(\mathbf{q})$  is enhanced only slightly since the three point vertex  $\Lambda$

for  $O_{xy}$ -quadrupole is much smaller. Figure 2 (d) gives the  $U$ -dependence of  $\alpha_0^c$  and  $\alpha_Q^c$  under the constraint  $J/U = 0.06$  in the SC-VC[c] method. Since the slope of  $\alpha_0^c$  is larger than that of  $\alpha_Q^c$ , the critical value  $(J/U)_c$  increases in the strong correlation region.

Now, we discuss the mechanism of the enhancement of  $\chi_{x^2-y^2}^c(\mathbf{0})$  in more detail: Considering the small inter-orbital mixing due to  $t'(\ll t)$ , we drop  $\chi_{ll',mm'}^{\text{irr},c}(\mathbf{0})$  in eq. (2) except for  $l = l' = m = m'$ . Then, eq. (2) is simplified to  $2 \times 2$  matrix equation with

$$\begin{aligned}\hat{\chi}^c(\mathbf{0}) &= \begin{pmatrix} \chi_{11,11}^c(\mathbf{0}) & \chi_{11,22}^c(\mathbf{0}) \\ \chi_{11,22}^c(\mathbf{0}) & \chi_{11,11}^c(\mathbf{0}) \end{pmatrix}, \\ \hat{\chi}^{\text{irr},c}(\mathbf{0}) &= \begin{pmatrix} \chi_{11,11}^{\text{irr},c}(\mathbf{0}) & 0 \\ 0 & \chi_{11,11}^{\text{irr},c}(\mathbf{0}) \end{pmatrix}, \\ \hat{\Gamma}^c &= - \begin{pmatrix} U & 2U' - J \\ 2U' - J & U \end{pmatrix}.\end{aligned}\quad (5)$$

For  $U' = U - 2J$ , the charge density susceptibility  $\chi_n^c(\mathbf{0}) = \sum_{l,m} \chi_c^{ll,mm}(\mathbf{0})$  and  $\chi_{x^2-y^2}^c(\mathbf{0})$  are obtained as

$$\begin{aligned}\chi_n^c(\mathbf{0}) &= 2\chi_{11,11}^{\text{irr},c}(\mathbf{0})(1 + (3U - 5J)\chi_{11,11}^{\text{irr},c}(\mathbf{0}))^{-1} \quad (6) \\ \chi_{x^2-y^2}^c(\mathbf{0}) &= 2\chi_{11,11}^{\text{irr},c}(\mathbf{0})(1 - (U - 5J)\chi_{11,11}^{\text{irr},c}(\mathbf{0}))^{-1} \quad (7)\end{aligned}$$

Therefore,  $\chi_{x^2-y^2}^c(\mathbf{0})$  is enhanced by Coulomb interaction when  $J/U < 0.2$ , while  $\chi_n^c(\mathbf{0})$  is always suppressed. If we drop the spin VC, the spin susceptibility is  $\chi^s(\mathbf{Q}) = 2\chi_{11,11}^0(\mathbf{Q})(1 - (U + J)\chi_{11,11}^0(\mathbf{Q}))^{-1}$ . Therefore, the relation  $\alpha_0^c > \alpha_Q^s$  holds for  $X_{11,11}^c(\mathbf{0}) > (U + J)\chi_{11,11}^0(\mathbf{Q})(U - 5J)^{-1} - \chi_{11,11}^0(\mathbf{0})$  for  $J/U < 0.2$ . Since  $X_{11,11}^{AL,c}(\mathbf{0})$  grows in proportion to  $T\chi^s(\mathbf{Q})[\log\{\chi^s(\mathbf{Q})\}]^2$  at high [low] temperatures [20],  $\chi_{x^2-y^2}^c(\mathbf{0})$  is strongly enhanced near the AFM-QC under the condition  $J/U \lesssim 0.2$ . This condition is expected to be satisfied in Ru-oxides.

Figure 2 (e) shows the  $J/U$ -dependence of  $\alpha_0^c$  and  $\alpha_Q^s$  given in the SC-VC[all] and SC-VC[c] methods, by adjusting  $U$  to satisfy  $\alpha_{\max} \equiv \max\{\alpha_{\max}^s, \alpha_{\max}^c\} = 0.97$ . In both methods, the obtained results are similar since  $\hat{X}^s$  is less important. The critical value of  $J/U$ , at which  $\alpha_0^c = \alpha_Q^s = 0.97$  is satisfied, is  $(J/U)_c = 0.095$  (0.086) in the SC-VC[all] (SC-VC[c]) method. Therefore, the relation  $\alpha_0^c > \alpha_Q^s$  is satisfied for  $J/U < (J/U)_c \sim 0.1$  in the present SC-VC method, in highly contrast to the PRA result  $(J/U)_c^{\text{PRA}} = 0$ ; see Fig. 1 (b).

Figure 3 shows (a)  $\chi^s(\mathbf{q})$  and (b)  $\chi_{x^2-y^2}^c(\mathbf{q})$  given by the SC-VC[all] method for  $U = 1.35$  and  $J/U = 0.06$ . The Stoner factors are  $\alpha_Q^s = 0.94$  and  $\alpha_0^c = 0.97$ . In this method, the shape of  $\chi^s(\mathbf{q})$  is slightly changed from the RPA result by the momentum dependence of  $\hat{X}^s(\mathbf{q})$ . However, the overall results of spin and quadrupole susceptibilities are unchanged by the spin VC. The obtained divergent behavior of  $\chi_{x^2-y^2}^c(\mathbf{0})$  is consistent with the “non-magnetic nematic phase” in  $\text{Sr}_3\text{Ru}_2\text{O}_7$  near the field-induced AFM-QC. Recent ultrasonic measurement

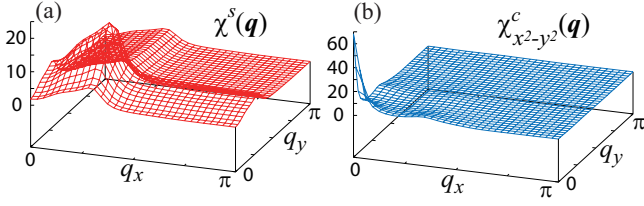


FIG. 3: (color online) (a)  $\chi^s(\mathbf{q})$  and (b)  $\chi^c_{x^2-y^2}(\mathbf{q})$  obtained by the SC-VC[all] method for  $U = 1.35$  and  $J/U = 0.06$ .

of the elastic constants reports a large softening of shear modulus  $C_S = (C_{11} - C_{12})/2$  under  $H_z \sim 7.8$  Tesla [24]. Since  $C_S^{-1} - C_{S,0}^{-1} \propto \chi^c_{x^2-y^2}(\mathbf{0})$  ( $C_{S,0}$  being the lattice shear modulus), the obtained development of  $\chi^c_{x^2-y^2}(\mathbf{0})$  in Fig. 3 (b) is consistent with experiment. We have verified that obtained results in Fig. 2 and 3 are qualitatively unchanged for  $3.1 \leq n \leq 3.6$ . We will report detailed  $n$  dependence of  $\chi^c_{x^2-y^2}$  and  $\chi^s$  in later publication.

The role of the AL term can be interpreted as the following effective nematic interaction within the mean-field picture:  $H_{\text{nem}} \sim g \sum_{\mathbf{k}, \mathbf{k}'} \hat{O}_{x^2-y^2}(\mathbf{k}) \hat{O}_{x^2-y^2}(\mathbf{k}')$ , where  $\hat{O}_{x^2-y^2}(\mathbf{k}) = \sum_{l,m,\sigma} O_{x^2-y^2}^{l,m} c_{\mathbf{k},l,\sigma}^\dagger c_{\mathbf{k},m,\sigma}$  and  $g$  is approximately given as  $(-U + 5J)(X_{11,11}^c(\mathbf{q}) + X_{22,22}^c(\mathbf{q}))/2\chi^0(\mathbf{q})$  at  $\mathbf{q} = \mathbf{0}$ , according to eq. (7). In previous studies of  $\text{Sr}_3\text{Ru}_2\text{O}_7$  based on the single-band model, on the other hand, the phenomenological Pomeranchuk interaction  $H'_{\text{nem}} \sim g' \sum_{\mathbf{k}, \mathbf{k}'} d_{\mathbf{k}} d_{\mathbf{k}'}$  had been frequently introduced, where  $d_{\mathbf{k}} = (\cos k_x - \cos k_y) \sum_{\sigma} c_{\mathbf{k},\sigma}^\dagger c_{\mathbf{k},\sigma}$ . They are similar in symmetry, since both  $d_{\mathbf{k}}$  and  $\hat{O}_{x^2-y^2}(\mathbf{k})$  belong to the same  $B_{1g}$  representation of  $D_{4h}$  point group. Thus, “orbital Pomeranchuk interaction” is driven by the AL-VC in multi-orbital models.

It is useful to comment on the difference between the present study and the study of the five-orbital model in Ref. [20]. In both models, we obtain the development of  $\chi^c_{x^2-y^2}(\mathbf{0})$  using the SC-VC method. In the latter model, in addition,  $\chi^c_{xz(yz)}(\mathbf{Q})$  also develops because of the VC and good *inter-orbital* ( $xz/yz-xy$ ) nesting. Both ferro- and antiferro-quadrupole fluctuations induce the *s*-wave superconductivity without sign reversal ( $s_{++}$ -wave state) [20]. On the other hand,  $\chi^c_{xz(yz)}(\mathbf{q})$  will be small in the  $t_{2g}$ -orbital model for Ru-oxides because of ill *inter-orbital* nesting. Thus, the results of this paper would be qualitatively unchanged in the three-orbital model.

Finally, we discuss the physical meaning of the VC in the strong-coupling regime ( $U \gg t$ ): Due to the Kugel-Khomskii type spin-orbital exchange coupling  $\sim (t^2/U)(\mathbf{s}_i \cdot \mathbf{s}_j)(O_{x^2-y^2}^i \cdot O_{x^2-y^2}^j)$ , the antiferro-spin order induces the ferro-orbital order, and vice versa. Such spin-orbital coupling should exist also in the metallic state ( $U \sim t$ ), and it is actually described by the AL-type VC. For this reason, cooperative development of spin and orbital fluctuations is obtained in the SC-VC anal-

ysis. [The RPA is insufficient in multi-orbital Hubbard models in that the spin-orbital coupling is completely ignored.] Especially, non-magnetic orbital nematic order can be realized since the scalar order parameter  $O_{x^2-y^2}$  is more stable than the vector order parameter  $\mathbf{s}$  against the quantum and thermal fluctuations.

In summary, we have studied the origin of non-magnetic nematic order in  $\text{Sr}_3\text{Ru}_2\text{O}_7$ , by applying the SC-VC method to the two-orbital Hubbard model. We have found that the present model exhibits the orbital Pomeranchuk instability near the magnetic quantum criticality, owing to the spin-orbital coupling described by the VC. For  $J/U < (J/U)_c \sim 0.1$ , the ferro-orbital order ( $\alpha_0^s \approx 1$ ) occurs prior to the magnetic transition ( $\alpha_Q^s \approx 1$ ). The present mechanism gives a natural explanation for the nematic order in  $\text{Sr}_3\text{Ru}_2\text{O}_7$  as well as Fe-based superconductors near AFM-QC, and it will be also realized in various multi-orbital models. As the origin of the field-induced AFM-QC. Both the van-Hove singularity [26, 27] and the field-suppression of quantum fluctuation [28] mechanisms had been discussed.

We note that the renormalization group (RG) method is very powerful for the study of VCs in low dimensional systems. Recently, the RG analysis has been performed for the  $(d_{xz}, d_{yz})$ -orbital Hubbard model [29], and revealed that  $\chi^c_{x^2-y^2}(\mathbf{0})$  is critically enhanced by both the magnetic and superconducting QCs.

This study has been supported by Grants-in-Aid for Scientific Research from MEXT of Japan. Part of numerical calculations were performed on the Yukawa Institute Computer Facility.

- 
- [1] O. Sakai *et al.*, J. Phys. Soc. Jpn. **66** (1997) 3005
  - [2] K. Matsuda *et al.*, Phys. Rev. Lett. **87**, 087203 (2001)
  - [3] R. Okazaki *et al.*, Science **331**, 439 (2011)
  - [4] M. Yi *et al.*, PNAS **108** 6878 (2011)
  - [5] S. Kasahara *et al.*, Nature **486**, 382 (2012)
  - [6] R.M. Fernandes *et al.*, Phys. Rev. Lett. **105**, 157003 (2010).
  - [7] T. Goto *et al.*, J. Phys. Soc. Jpn. **80**, 073702 (2011).
  - [8] M. Yoshizawa *et al.*, Phys. Soc. Jpn. **81**, 024604 (2012).
  - [9] S. A. Grigera *et al.*, Science **294**, 329 (2001)
  - [10] R. A. Borzi *et al.*, Science **315**, 214 (2007).
  - [11] K. Kitagawa *et al.*, Phys. Rev. Lett. **95**, 127001 (2005).
  - [12] A.P. Mackenzie *et al.*, Physica C **481**, 207 (2012).
  - [13] C.J. Halboth and W. Metzner, Phys. Rev. Lett. **85**, 5162 (2000).
  - [14] C. Honerkamp, Phys. Rev. B **72**, 115103 (2005).
  - [15] Y. Yoshioka and K. Miyake, J. Phys. Soc. Jpn. **81**, 023707 (2012).
  - [16] S. Raghu *et al.*, Phys. Rev. B **79**, 214402 (2009).
  - [17] W.-C. Lee and C. Wu, Phys. Rev. B **80**, 104438 (2009).
  - [18] K. W. Lo *et al.*, arXiv:1207.4206.
  - [19] C. Fang *et al.*, Phys. Rev. B **77**, 224509 (2008).
  - [20] S. Onari and H. Kontani, Phys. Rev. Lett. **109**, 137001 (2012).

- [21] H. Kontani *et al.*, Solid State Communications, **152** (2012) 718.
- [22] H. Kontani *et al.*, Phys. Rev. B **75**, 184416 (2007); H. Kontani *et al.*, Phys. Rev. Lett. **100**, 096601 (2008).
- [23] T. Moriya, *Spin Fluctuations in Itinerant Electron Magnetism* (Springer-Verlag, 1985); A. Kawabata: J. Phys. F **4** (1974) 1477.
- [24] T. Suzuki, private communication.
- [25] P. Jakubczyk *et al.*, Phys. Rev. Lett. **103**, 220602 (2009);
- [26] H. Yamase and A.A. Katanin, J. Phys. Soc. Jpn. **76**, 073706 (2007).
- [27] M.H. Fischer and M. Sigrist, Phys. Rev. B **81**, 064435 (2010).
- [28] K. Sakurazawa *et al.*, J. Phys. Soc. Jpn. **74** (2005) 271.
- [29] M. Tsuchiizu, S. Onari, and H. Kontani, arXiv:1209.3664.